

# Fabrication and magnetic properties of amorphous $\text{Co}_{0.71}\text{Pt}_{0.29}$ nanowire arrays

Hua Li<sup>a</sup>, Cailing Xu<sup>a</sup>, Guangyu Zhao<sup>a</sup>, Yikun Su<sup>a</sup>, Tao Xu<sup>b</sup>, Hulin Li<sup>a,\*</sup>

<sup>a</sup>College of Chemistry and Chemical Engineering, Lanzhou University, Lanzhou 730000, P.R. China

<sup>b</sup>State Key Laboratory of Solid Lubrication, Lanzhou Institute of Chemical Physics, Chinese Academy of Science, Lanzhou 730000, P.R. China

Received 14 May 2004; received in revised form 23 June 2004; accepted 29 July 2004 by C.E.T. Gonçalves da Silva

Available online 14 August 2004

## Abstract

Highly ordered  $\text{Co}_{0.71}\text{Pt}_{0.29}$  alloy nanowire arrays have been fabricated successfully by direct current electro-deposition into the pores of a porous anodic aluminum oxide (AAO) template. SEM and TEM images reveal that the nanowires of array are uniform, well isolated, and parallel to one another. The aspect ratio of nanowires is over 200. XRD and EDS pattern indicates that amorphous  $\text{Co}_{0.71}\text{Pt}_{0.29}$  structure was formed during electro-deposition. In amorphous sample, magnetocrystal anisotropy is very small, therefore, shape anisotropy plays a dominant role which leads to strong perpendicular anisotropy. High coercivity ( $H_c = 1.7$  kOe) and squareness ( $M_r/M_s$ ) around 0.7 were obtained in the samples when the field was applied parallel to the axis of the nanowires. However, when it changed to polycrystalline structure after annealing, due to the competition of magnetocrystal anisotropy and shape anisotropy, the sample did not display perpendicular anisotropy.

© 2004 Elsevier Ltd. All rights reserved.

PACS: 75.30.Gw; 75.50.Ss; 75.60.Ej; 82.45.Qr

Keywords: A.  $\text{Co}_{0.71}\text{Pt}_{0.29}$  nanowire arrays; B. Magnetic recording materials; D. AAO template

## 1. Introduction

One-dimensional (1D) nanostructured materials, such as nanorods and nanowires, have attracted much attention due to their novel chemical and physical properties [1]. In particular, 1D magnetic nanomaterials have been extensively exploited not only for the fundamental interest but also for their potential utilization in ultrahigh-density magnetic storage devices [2,3], magneto-optic recording media [4–6] and spintronics [7–10]. However, the most of the work on 1D magnetic nanomaterial have been mainly focused on the polycrystalline structure alloy [11–14]. To

our best knowledge, fabrication and magnetic properties of 1D amorphous binary alloy magnetic nanomaterial have not been reported so far. But in some polycrystalline sample, due to the competition between magnetocrystalline anisotropy and shape anisotropy, there may be no perpendicular anisotropy [15,16]. Since the magnetic properties of nanowire arrays are related to their element components, morphology and microstructures [17], 1D amorphous magnetic nanoalloy are expected to exhibit the perpendicular anisotropy. Besides, the amorphous magnetic nanomaterials seem to be more suitable candidates for magneto-optic recording media than crystalline magnetic nanomaterials because of low medium noise and high signal-to-noise ratio. Polycrystalline nanomaterials are formed by small crystals, so boundaries between these small crystals will be sure to cause noise of the crystal boundary when polycrystalline nanomaterials are subjected to read/write operations. In contrast, amorphous magnetic materials can

\* Corresponding author. Tel.: +86-931-891-2517; fax: +86-931-891-2582.

E-mail addresses: [huali@lzu.edu.cn](mailto:huali@lzu.edu.cn) (H. Li), [lih@lzu.edu.cn](mailto:lih@lzu.edu.cn) (H.L. Li).

avoid noise of the crystal boundary because of their amorphous microstructures. Although the key synthetic methodologies of 1D magnetic nanomaterials developed so far include catalyzed high-temperature growth via the vapor–liquid–solid (VLS) mechanism [18,19], molecular beam epitaxy [20], ion-beam irradiation [21], it remains a challenge to prepare high perpendicular magnetic anisotropy and coercivity magnetic nanowires without high vacuum, application of pressure, supply of temperature and external magnetic field applied during electro-deposition. Here, we report the first successful synthesis of an interesting 1D amorphous magnetic  $\text{Co}_{0.71}\text{Pt}_{0.29}$  alloy with obvious perpendicular anisotropy by direct current electro-deposition into the pores of a porous anodic aluminum oxide (AAO) template at room temperature and normal pressure. The advantages of this method in the production of high perpendicular magnetic anisotropy nanowires are obvious because of its simplicity, convenience, and capability of producing large quantities of samples. Furthermore, the amorphous  $\text{Co}_{0.71}\text{Pt}_{0.29}$  alloy nanowire arrays obtained with a strong perpendicular magnetic anisotropy, high coercivity, large magneto-optic Kerr effect and a low medium noise are among the most interesting candidates for ultra-high-density recording and magneto-optic recording media.

## 2. Experiment

Highly ordered AAO templates with pore diameter of about 50 nm were prepared by anodic oxidation of 99.999% pure Al sheet in oxalic acid solution under two-step anodizing process [22,23]. The first process was carried out at a constant voltage of 40 V in 0.3 M oxalic acid solution at 10–15 °C for 3 h. Secondly, the oxide film was dissolved in 0.4 M  $\text{H}_3\text{PO}_4$ , 0.2 M  $\text{H}_2\text{Cr}_2\text{O}_4$  at 50 °C. Then, the anodization was performed for 10 h under the same condition as the first one. The as-prepared template was dipped into 5% phosphoric acid at 50 °C for 20 min to eliminate the obstacle film, and then a silver film of 300 nm thick was sputtered onto one side of the template to act as a conductive contact.

Electro-deposition was carried out at room temperature, using a three-electrode potentiostatic control and direct current electro-deposition system with a saturated calomel electrode (SEC) as reference electrode, a 1 cm × 0.5 cm platinum plate as a counter electrode and the Ag coated AAO template as working electrode. The  $\text{Co}_{0.71}\text{Pt}_{0.29}$  nanowires used in the experiments described here were grown from a solution of  $[\text{CoSO}_4] = 1.2 \text{ mol dm}^{-3}$ ,  $[\text{K}_2\text{PtCl}_6] = 0.012 \text{ mol dm}^{-3}$ ,  $[\text{H}_3\text{BO}_4] = 30\text{--}40 \text{ g dm}^{-3}$ , pH 2.0–3.0 at  $-0.8 \text{ V}$  (vs. SCE).

After electro-deposition, the sample was annealed at 700 °C for 20 min in Ar (999.999%) atmosphere (heating rate: 100 °C/min, cooling rate: 100 °C/min).

To obtain the SEM image of the  $\text{Co}_{0.71}\text{Pt}_{0.29}$  nanowire arrays, the sample was dipped into a solution of 6%  $\text{H}_3\text{PO}_4$

and 1.8%  $\text{H}_2\text{CrO}_4$  at 50 °C for 30 min to dissolve the alumina matrix partly and washed by distilled water several times. For TEM imaging, we dipped the as prepared samples into 6%  $\text{H}_3\text{PO}_4$  and 1.8%  $\text{H}_2\text{CrO}_4$  at 50 °C for 180 min to dissolve the AAO completely.

### 2.1. Instruments

The morphology of the AAO templates was examined by atomic force microscopy (AFM). Transmission electron microscopy (TEM, Hitachi 600) and scanning electron microscopy (SEM, JEOL JSM-5600LV) were used to characterize the morphology of nanowire arrays. The crystalloid structure of the samples was determined by X-ray diffraction (XRD, Rigaku, Model D/max 2400; Cu  $K\alpha$  radiation,  $\lambda = 1.54056 \text{ \AA}$ ). The average composition of the nanowires was measured from energy dispersive spectra (EDS). Magnetic properties of the as-prepared and annealing samples were tested by a vibrating sample magnetometer (VSM, TOEI-5S-15).

## 3. Results and discussion

For AAO film, its micrography was investigated by AFM. The results indicate that the diameter and interpore distances (center to center) are about 50 and 75 nm, respectively, and pore densities about  $10^{10} \text{ cm}^{-2}$  in the resulting AAO template prepared by two-step anodization (see Fig. 1). Generally, the higher the anodized voltage is, the larger the pore diameter of AAO film is; the longer the time is, the thicker the film is and the deeper the pores are.

Fig. 2 shows the SEM images of the as-grown  $\text{Co}_{0.71}\text{Pt}_{0.29}$  nanowires. As can be seen from a low-magnification SEM image (Fig. 2a), the sample consists of a large quantity of straight nanowire arrays, no other morphologies are observed in the product. Fig. 2b is a cross-

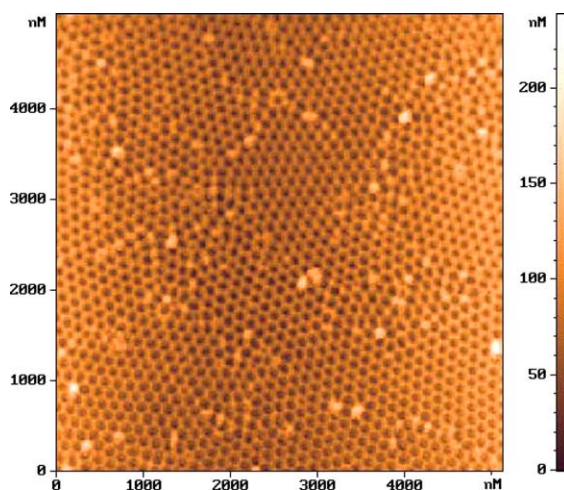


Fig. 1. AFM image of AAO template.

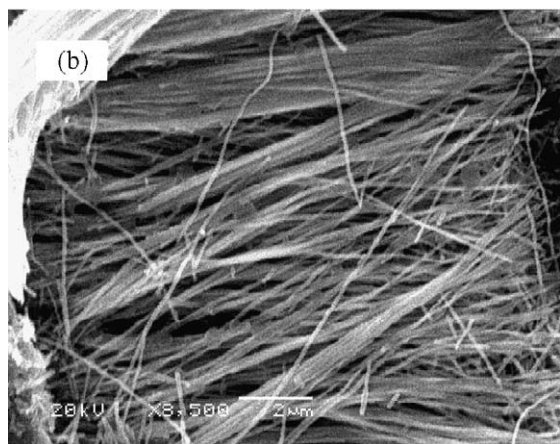
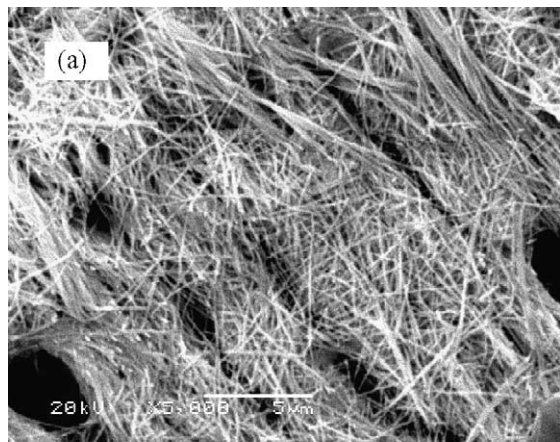


Fig. 2. SEM images of uniform  $\text{Co}_{0.71}\text{Pt}_{0.29}$  nanowires that were prepared via the electro-deposition. The wires have lengths along the longitudinal axis of up to 10  $\mu\text{m}$ . (a) view from the top; (b) view from the side.

sectional image of  $\text{Co}_{0.71}\text{Pt}_{0.29}$  nanowire arrays prepared by electro-deposition for 3 h. One can see that the nanowires of array are very uniform, well isolated and parallel to each other. Some wires bend together when released partly from AAO template, which may be due to internal stress during electro-deposition. The average length of the as-deposited  $\text{Co}_{0.71}\text{Pt}_{0.29}$  nanowires is about 10  $\mu\text{m}$ . The lengths of the nanowires can be controlled from several nm to 20  $\mu\text{m}$  according to deposition time. TEM images of the as-prepared  $\text{Co}_{0.71}\text{Pt}_{0.29}$  nanowires are shown in Fig. 3. The nanowires prepared by AAO template synthesis are of regular size and are continuous. All of them have uniform diameter of about 50 nm, which basically equals to that of pores of the AAO template. However, in the TEM picture nanowires also appear irregular and they show different contrast within themselves. This can be explained by that nanowires are formed by small particles with different composition. The average length of  $\text{Co}_{0.71}\text{Pt}_{0.29}$  nanowires

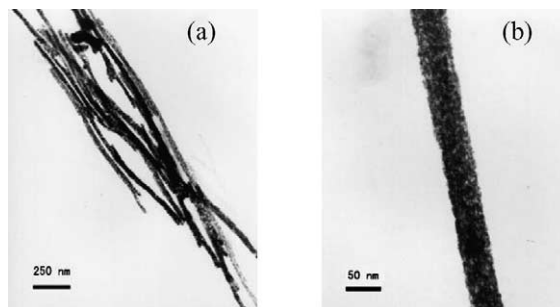


Fig. 3. TEM images of (a) several  $\text{Co}_{0.71}\text{Pt}_{0.29}$  nanowires, (b) a single  $\text{Co}_{0.71}\text{Pt}_{0.29}$  nanowire with 50 nm in diameter.

prepared by electro-deposition for 1 h is above 10  $\mu\text{m}$  and the typical diameter is about 50 nm, i.e. the aspect ratio is above 200. Hence, the shape anisotropy of  $\text{Co}_{0.71}\text{Pt}_{0.29}$  nanowire arrays is very high in our case.

Fig. 4 shows an EDS pattern of the  $\text{Co}_{0.71}\text{Pt}_{0.29}$  nanowire arrays produced by dc electro-deposition at  $-0.8$  V. The average composition of the nanowire arrays was 70.69 at.% Co, 29.31 at.% Pt. The EDS pattern also shows the peaks of element Al, which is attributed to the AAO template. The XRD scans were performed to examine the crystal structure of the  $\text{Co}_{0.71}\text{Pt}_{0.29}$  alloy nanowire arrays. The typical diffraction pattern is shown in Fig. 5b, from which we can see that no obvious reflection peak was found, indicating amorphous-like structure of as-deposited. Whether the deposit is amorphous or crystalline depends on the growth conditions such as applied voltage, electrolyte concentration and so on [24]. After annealing at 700  $^{\circ}\text{C}$  for 20 min in 99.999% Ar, the diffraction peaks are found at 39.70 $^{\circ}$ , 46.42 $^{\circ}$ , 67.58 $^{\circ}$  and 81.27 $^{\circ}$ , corresponding to the (1 1 1), (2 0 0), (2 2 0) and (3 1 1) planes of fcc CoPt structure (see Fig. 5a). From Fig. 5(a) and (b), we can clearly see that upon anneal treatment, the  $\text{Co}_{0.71}\text{Pt}_{0.29}$  nanowires changed its original amorphous phase to stable polycrystalline structure. Shown in Fig. 6 is the Differential temperature analysis (DTA) pattern of amorphous  $\text{Co}_{0.71}\text{Pt}_{0.29}$  nanowire arrays. DTA curve shows a strong exothermic reaction, implying the process of crystallization of the amorphous  $\text{Co}_{0.71}\text{Pt}_{0.29}$  nanowire.

Fig. 7(a) and (b) show magnetization hysteresis loops at room temperature of as-deposited and annealed samples, respectively, under a field applied parallel or perpendicular

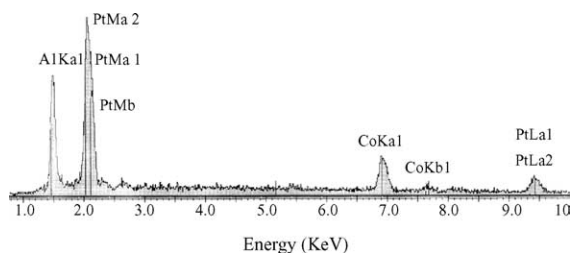


Fig. 4. EDS pattern of the CoPt alloy nanowires. The composition ratio of the nanowires was 70.69 at.% Co, 29.31 at. % Pt.

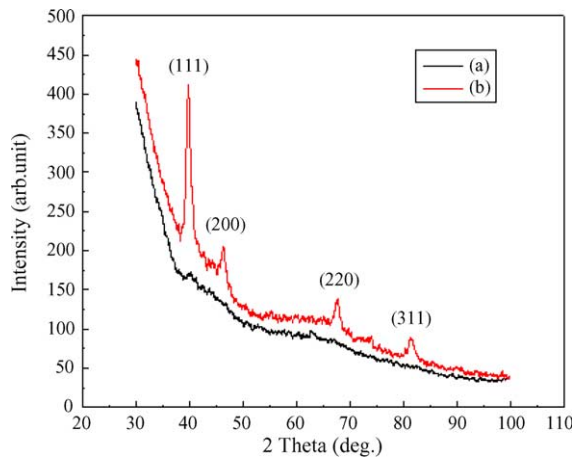


Fig. 5. X-ray diffraction patterns of  $\text{Co}_{0.71}\text{Pt}_{0.29}$  nanowire arrays (a) as-deposited, (b) annealed at  $700\text{ }^\circ\text{C}$  for 20 min in 99.999% Ar.

to the length axis of the wires. As can be seen, the coercivity and squareness ( $M_r/M_s$ ) of as-prepared are about 1.7 kOe and 0.7, respectively, when the field applied is parallel to the axis of nanowires arrays, much larger than the coercivity (800 Oe) and squareness ( $M_r/M_s=0.3$ ) when the field applied is perpendicular to the nanowire arrays, indicating that the easily magnetized direction of  $\text{Co}_{0.71}\text{Pt}_{0.29}$  nanowire arrays is parallel to the nanowire arrays and that it has obvious magnetic anisotropy. Under conditions of small diameters about 50 nm and aspect ratio above 200, the  $\text{Co}_{0.71}\text{Pt}_{0.29}$  nanowires behave like a single domain structure. In Fig. 7b, the squareness for the loops measured in parallel and perpendicular to fields are 0.3 and 0.4, respectively, implying a weak in-plane magnetic anisotropy. These different magnetic behaviors before and after annealing can be attributed to their different microstructures. XRD patterns indicate that the annealed samples grow preferentially along the (1 1 1) crystal direction, i.e. perpendicular to nanowire (in-plane). When only magnetocrystalline anisotropy is considered, the preferred direction

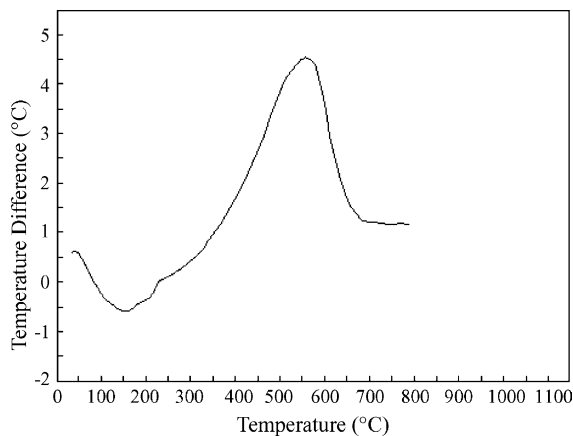


Fig. 6. DTA pattern of  $\text{Co}_{0.71}\text{Pt}_{0.29}$  nanowire arrays.

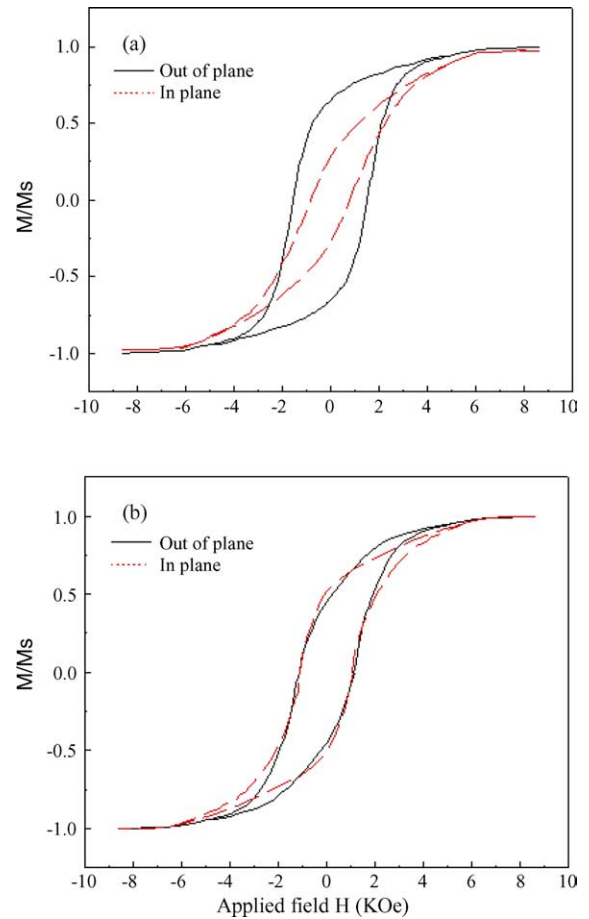


Fig. 7. The magnetization hysteresis loops at room temperature (a) as-deposited, (b) annealed at  $700\text{ }^\circ\text{C}$  for 20 min in 99.999% Ar. (Out of plane means applied field is parallel to the nanowires; in plane means field perpendicular to the nanowires).

(1 1 1) of the annealed  $\text{Co}_{0.71}\text{Pt}_{0.29}$  nanowire arrays is easy to magnetize. When shape anisotropy is also considered, the result of the competition between magnetocrystalline anisotropy and shape anisotropy is that magnetocrystalline anisotropy is a little stronger than shape anisotropy, so the sample displays a weak in-plane magnetic anisotropy. XRD evidences show that the sample before annealing is amorphous, but it changes to be polycrystalline after annealing. For polycrystalline sample, magnetocrystalline anisotropy ( $k_\mu \sim 5 \times 10^5 \text{ J/m}^3$ ) is comparable with the shape anisotropy ( $(\mu_0 M_s^2/4) \sim 1 \times 10^5 \text{ J/m}^3$  for infinite cylinder), as a result, the competition of the two kinds of anisotropy energies results in no perpendicular anisotropy of sample B. But for amorphous  $\text{Co}_{0.71}\text{Pt}_{0.29}$  nanowires of sample A, magnetocrystalline anisotropy is very weak, therefore, shape anisotropy makes the main contribution for total anisotropy which favors the magnetization perpendicular to the film plane (along the wire axis). Zeng et al. [25] also pointed out that the magnetic reversal mechanism may be

attributed to localized nucleation in such case, which will decrease the shape anisotropy. Upon annealing the effects of crystallization cause the decrease of superior perpendicular magnetic characteristics for  $\text{Co}_{0.71}\text{Pt}_{0.29}$  nanowires. But for as-prepared, the competition between shape anisotropy and magnetocrystal anisotropy is unlikely to occur, because the latter contribution does not exist due to the amorphous structure of these  $\text{Co}_{0.71}\text{Pt}_{0.29}$  nanowires. Since a unit cell of magnetic nanowire arrays acts as a recording cell [26], the nanowire arrays fabricated by porous alumina film containing  $10^{10}$  cells per square centimeter have a striking magnetic recording density about (60Gbit/in<sup>2</sup>). Therefore, the electro-deposited amorphous magnetic recording nanowire arrays are promising for producing perpendicular magnetic recording medium with a super-high density and magneto-optic recording media. The magnetic properties of amorphous CoPt alloy nanowire arrays with different diameter and different annealing temperature will be reported in our later work.

To summarize, highly ordered amorphous  $\text{Co}_{0.71}\text{Pt}_{0.29}$  nanowire arrays have been fabricated successfully by direct current electro-deposition into the pores of a porous AAO template. Magnetization measurement on the arrays of amorphous  $\text{Co}_{0.71}\text{Pt}_{0.29}$  nanowires demonstrated a notable perpendicular magnetic anisotropy, which are mainly attributed to shape anisotropy. Crystallization of the sample causes the decrease of superior perpendicular magnetic characteristics for  $\text{Co}_{0.71}\text{Pt}_{0.29}$  nanowires. The study of amorphous alloy nanowires leads to striking and yet fairly understood differences from the better-known 1D crystalline structure.

### Acknowledgements

We thank the National Natural Science Foundation of China (Grant No: 60171004).

### References

- [1] Y.N. Xia, P.D. Yang, Y.G. Sung, et al., *Adv. Mater.* 15 (2003) 353.
- [2] C.J. Murphy, N.R. Jana, *Adv. Mater.* 14 (2002) 80.
- [3] N. Cordente, M. Respaud, F. Senocq, et al., *Nano Lett.* 10 (2001) 565.
- [4] D. Weller, H. Brändle, C. Chappert, *J. Magn. Magn. Mater.* 121 (1993) 461.
- [5] S. Hashimoto, Y. Ochiai, K. Aso, *J. Appl. Phys.* 66 (1989) 4909.
- [6] Y. Peng, T.-H. Shen, B. Ashworth, *Appl. Phys. Lett.* 83 (2003) 2.
- [7] D.J. Sellmyer, M. Zheng, R. Skomski, *J. Phys.: Condens. Mater.* 13 (2001) R433.
- [8] A. Fert, L. Piraux, *J. Magn. Magn. Mater.* 200 (1999) 338.
- [9] R.J. Tonucci, B.L. Justus, A.J. Campillo, C.E. Ford, *Science* 258 (1992) 783.
- [10] T.W. Whitney, J.S. Jiang, P.C. Searson, C.L. Chien, *Science* 261 (1993) 1316.
- [11] W. Chen, S.L. Tang, M. Lu, Y.W. Du, *J. Phys.: Condens. Mater.* 15 (2003) 4623.
- [12] A.J. Yin, J. Li, W. Jian, et al., *Appl. Phys. Lett.* 79 (2001) 1039.
- [13] S. Park, S. Kim, S. Lee, et al., *J. Am. Chem. Soc.* 22 (2000) 8581.
- [14] Y.W. Wang, G.W. Meng, C.H. Ling, et al., *Chem. Phys. Lett.* 343 (2001) 174.
- [15] L. Piraux, S. Dubois, E. Ferain, *J. Magn. Magn. Mater.* 165 (1997) 352.
- [16] P.M. Paulus, F. Luis, M. Kröll, G. Schmid, L.J. de Jongh, *J. Magn. Magn. Mater.* 224 (2001) 180.
- [17] X.Y. Yuan, G.S. Wu, T. Xie, *Solid State Commun.* 130 (2004) 429.
- [18] A.M. Morales, C.M. Lieber, *Science* 279 (1998) 208.
- [19] P.M. Ajayan, *Chem. Rev.* 99 (1999) 1787.
- [20] G.R. Harp, D. Weller, T.A. Rabedeau, et al., *Phys. Rev. Lett.* 71 (1993) 2493.
- [21] S.P. Withrowa, C.W. Whitea, J.D. Budai, *J. Magn. Magn. Mater.* 260 (2003) 319.
- [22] D.H. Qin, M. Lu, *Chem. Phys. Lett.* 350 (2001) 51.
- [23] S. Yang, H. Zhu, D. Yu, Z. Jin, S. Tang, Y. Du, *J. Magn. Magn. Mater.* 222 (2000) 97.
- [24] U. Admon, M.P. Dariel, E. Grunbaum, *J. Appl. Phys.* 59 (1986) 2003.
- [25] H. Zeng, M. Zheng, R. Skomski, D.J. Sellmyer, *J. Appl. Phys.* 87 (2000) 4718.
- [26] H. Daimon, O. Knakami, O. Iangoya, A. Sakemoto, *Jpn. J. Appl. Phys.* 132 (1991) 282.